

Prequential posteriors

Shreya Sinha Roy
 Richard G. Everitt
 Christian P. Robert*
 Ritabrata Dutta

*Department of Statistics, University of Warwick
 Coventry, CV4 7AL
 United Kingdom*

SHREYA.SINHA-ROY@WARWICK.AC.UK
 RICHARD.EVERITT@WARWICK.AC.UK
 C.A.M.ROBERT@WARWICK.AC.UK
 RITABRATA.DUTTA@WARWICK.AC.UK

Abstract

Data assimilation is a fundamental task in updating forecasting models upon observing new data, with applications ranging from weather prediction to online reinforcement learning. Deep generative forecasting models (DGFMs) have shown excellent performance in these areas, but assimilating data into such models is challenging due to their intractable likelihood functions. This limitation restricts the use of standard Bayesian data assimilation methodologies for DGFMs. To overcome this, we introduce *prequential posteriors*, based upon a predictive-sequential (prequential) loss function; an approach naturally suited for temporally dependent data which is the focus of forecasting tasks. Since the true data-generating process often lies outside the assumed model class, we adopt an alternative notion of consistency and prove that, under mild conditions, both the prequential loss minimizer and the prequential posterior concentrate around parameters with optimal predictive performance. For scalable inference, we employ easily parallelizable wastefree sequential Monte Carlo (SMC) samplers with preconditioned gradient-based kernels, enabling efficient exploration of high-dimensional parameter spaces such as those in DGFMs. We validate our method on both a synthetic multi-dimensional time series and a real-world meteorological dataset; highlighting its practical utility for data assimilation for complex dynamical systems.

1 Introduction

Data assimilation (Vetra-Carvalho et al., 2018) refers to the process of combining observational data with a computational model to estimate the evolving state of a dynamical system. It plays a crucial role in domains such as weather forecasting, meteorology, climate modeling, sequential decision-making, and online reinforcement learning. A standard approach for modeling time series data, keeping data assimilation feasible, is through state space models (SSMs). In SSMs, the latent state evolves according to a dynamic model, coupled with an observational error model. Under the classical assumption of Gaussian errors and linear dynamics, inference can be performed via the Kalman filter. However, this setting is insufficient for nonlinear and complex dynamics, leading to extensions such as the extended Kalman filter (EKF) (Ribeiro, 2004) and the ensemble Kalman filter (EnKF) Evensen (2003). On the other hand the physics-based partial differential equation models (Fisher et al., 2009) are the work horse of the weather community, but data-assimilation

*. Also affiliated with CEREMADE, Université Paris Dauphine PSL, France

for them tend to be computationally expensive. In the weather forecasting community, variational approaches such as 3D-Var and 4D-Var (Courtier et al., 1998; Andersson et al., 1994) have been proposed as optimization-based filtering and smoothing algorithms, but their computational cost is often prohibitive.

Recent years have seen a surge of DNN-based models (Arcucci et al., 2021; Qu et al., 2024) providing fast, low-cost simulations and capturing complex nonlinear dynamics, as alternatives to numerical weather prediction (NWP) models. Prominent deterministic forecasting systems include Pangu-Weather (Bi et al., 2022), FourCastNet (Pathak et al., 2022), GraphCast (Lam et al., 2023) and ClimaX (Nguyen et al., 2023). These models, typically trained with mean squared error (MSE) losses or their variants, achieve impressive accuracy but fail to provide uncertainty quantification. To address this limitation, deep generative forecasting models (DGFMs) such as GenCast (Price et al., 2024) employ generative modeling for uncertainty-aware forecasts. While adversarial training is common in generative modeling, Pacchiardi et al. (2024a) demonstrate that proper scoring rules (SRs) (Gneiting and Raftery, 2007; Waghmare and Ziegel, 2025) can yield calibrated probabilistic forecasts without adversarial objectives from DGFMs. This has also been adapted for training of DGFMs used for probabilistic forecasting by the European centre for midrange weather forecasting (ECMWF) (Lang et al., 2024).

A central challenge in implementing Bayesian data assimilation for DGFMs is the lack of a tractable likelihood function, which is fundamental to classical Bayesian inference. Likelihood-free approaches such as approximate Bayesian computation (ABC) (Lintusaari et al., 2017; Bernton et al., 2019) and synthetic likelihood (Price et al., 2018; An et al., 2020; Dutta et al., 2016) exploit model simulation to define a posterior, but face scalability issues. Alternatively, generalized posteriors based on loss function (Bissiri et al., 2016; Jewson et al., 2018; Knoblauch et al., 2022) provide a more flexible framework for probabilistic inference with generative models. Recent work by Pacchiardi et al. (2024b) extends this framework to deep generative models by defining posteriors over neural network parameters. However, while such loss-based methods are well studied for the independent and identically distributed (IID) data setting, their extension to time-dependent data remains limited; leaving a gap in applying data assimilation for generative models.

In this work, we address this gap by introducing the notion of a *prequential posterior* for data assimilation. Instead of relying on the (often unavailable) likelihood, we replace it with a prequential loss (Dawid, 1991, 1992; Dawid and Vovk, 1999), which directly evaluates predictive performance on sequential data. This formulation is especially well suited for probabilistic forecasting, where the objective is not only to achieve accurate predictions but also to quantify predictive uncertainty. However, this raises a fundamental issue: the true data-generating process is rarely contained within the assumed model class. Under such model misspecification, classical consistency results (e.g., convergence of the MLE to the true parameter) no longer apply.

To overcome this, we adopt a different notion of predictive consistency (Skouras and Dawid, 2000), which focuses on selecting the parameter that minimizes the one-step-ahead predictive risk rather than recovering a nonexistent “true” parameter. We show that the minimizer of the empirical prequential loss is consistent in this predictive sense and establish a Bernstein–von Mises-type result for the generalized prequential posterior, demonstrating concentration around the optimal predictive parameter.

Sequential Monte Carlo (SMC) methods (Del Moral et al., 2006) have been widely used for data assimilation across domains such as geosciences, engineering, and machine learning, with applications ranging from earthquake forecasting (Werner et al., 2011) to online reinforcement learning (Roy et al., 2024). In this work, we implement an easily parallelizable, waste-free SMC algorithm (Dau and Chopin, 2022), equipped with a gradient-based, preconditioned forward kernel to ensure efficient exploration of high-dimensional parameter spaces. This kernel is inspired by stochastic gradient Markov chain Monte Carlo (SG-MCMC) methods (Welling and Teh, 2011; Chen et al., 2014; Ding et al., 2014) and adaptive stochastic methods (Jones and Leimkuhler, 2011), where particle transitions are guided by gradient information. Additionally, we incorporate RMSprop-style preconditioning (Chen et al., 2016) to enhance stability and performance in high-dimensional settings.

Together, these components form a likelihood-free, scalable, and adaptive Bayesian framework for data assimilation using DGFMs. The main contributions of our work are summarized below:

1. A likelihood-free data assimilation framework for deep generative forecasting models (DGFMs) via prequential posteriors.
2. Theoretical analysis of the prequential posterior, establishing predictive consistency under model misspecification.
3. A scalable and computationally efficient SMC algorithm for training high-dimensional neural network parameters.

The remainder of the paper is structured as follows. Section 2 introduces the posterior formulation and presents an asymptotic analysis in Section 2.2 using a different notion of consistency for a generic loss function. In Section 2.3, we introduce scoring rules as a special class of loss functions, which we use to define the prequential posterior. Our proposed sequential inference method via SMC is described in Section 3. Section 4 presents our simulation studies, where we compare our data assimilation method with a misspecified ensemble Kalman filter (EnKF) for a time series model called Lorenz 96 (Lorenz, 1996) and demonstrate its superior long-run predictive performance. We also apply the approach to a real-world meteorological forecasting task using the WeatherBench dataset (Rasp et al., 2020). We conclude in Section 5, where we summarize our findings and discuss potential directions for future research.

2 Prequential posterior for data-assimilation of DGFMs

Consider a discrete-time stochastic process (Y_1, Y_2, \dots) , where each $Y_t \in \mathcal{Y} \subseteq \mathbb{R}^l$. We assume that these random variables are not independent; rather, they exhibit temporal dependencies. Suppose that the true underlying process generating the observations is denoted by P . Given that the observations exhibit temporal dependence, it is reasonable to assume that the distribution of the observation at time t depends on the entire history of observations up to time $t - 1$. Formally, we express this by stating that

$$Y_t \sim P_t, \quad \text{where } P_t = P(\cdot \mid Y_{1:t-1}),$$

where we use the notation $Y_{i:j}$ to denote the sequence of observations Y_i, Y_{i+1}, \dots, Y_j .

Deep generative forecasting models (DGFMs) Probabilistic forecasting seeks not only accurate predictions of future observations but also reliable uncertainty estimates. A common way to achieve this is via a *simulator model* Q^θ that generates forecasts at time t from past data $Y_{1:t-1}$:

$$\hat{Y}_t \sim Q_t^\theta, \quad \theta \in \Theta \subseteq \mathbb{R}^p.$$

If the true data-generating distribution P lies in the model class $\mathcal{Q} = \{Q^\theta : \theta \in \Theta\}$, then the model is *well-specified*, with some θ^* satisfying $Q^{\theta^*} = P$. Deep generative models provide a natural choice for Q^θ , as they can capture nonlinear, high-dimensional dynamics while producing samples rather than point predictions. In this case, the forecast is generated by pushing auxiliary randomness W through a neural network:

$$\hat{Y}_t = Q^\theta(Y_{1:t-1}, W),$$

where W is independent noise and θ are the network parameters. We refer to this class of models as *deep generative forecasting models (DGFMs)*, which combine the expressiveness of deep learning with uncertainty-aware simulation for forecasting tasks (Price et al., 2024; Pacchiardi et al., 2024a).

Bayesian inference on these model parameters typically requires a tractable likelihood function, which poses a significant challenge in the context of generative models. Pacchiardi et al. (2024b) provided a likelihood-free framework for Bayesian inference for deep generative models. We extend this work to settings with *temporal dependencies* in the observations, drawing inspiration from the prequential framework proposed by Dawid (1991), Dawid (1984), Dawid (1992), Dawid and Vovk (1999).

2.1 Prequential posteriors

Let the sequence of random variables $Y = (Y_1, Y_2, \dots)$ be defined on a complete filtered probability space $(\Omega, \mathcal{F}, (\mathcal{F}_t), P)$, where each Y_t is \mathcal{F}_t -measurable and the filtration \mathcal{F}_t is the σ -algebra generated by $Y^t = (Y_1, Y_2, \dots, Y_t)$.

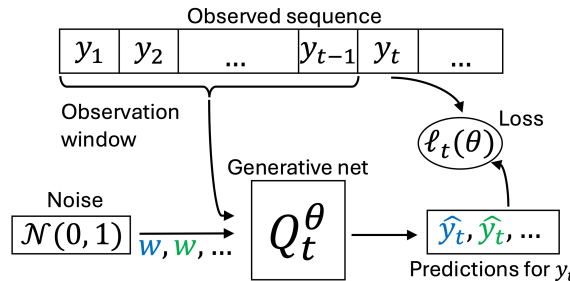


Figure 1: Illustration of the loss calculation. The loss function ℓ_T^θ evaluates forecasts generated by the conditional generative network Q_t^θ , which predicts Y_t given the past observations $Y_{1:t-1}$; with respect to the observed y_t .

We assign a time-indexed, \mathcal{F}_t -measurable loss function $\ell_t(\theta)$ to the simulator model Q_t^θ , which produces a forecast \hat{Y}_t at time t . This loss function evaluates the discrepancy between the forecast \hat{Y}_t and the actual observation Y_t , conditioned on the past observations $Y_{1:t-1}$ as shown in Figure 1.

Given an observed sequence $Y^T = (Y_1, Y_2, \dots, Y_T)$, we define the *prequential (predictive sequential)* loss for the simulator model Q^θ as

$$L_T(\theta) = \sum_{t=1}^T \ell_t(\theta).$$

Thus, $L_T(\theta)$ is a \mathcal{F}_T -measurable loss which assesses the predictive performance of the model Q^θ with respect to the sequence of observations Y^T .

Let us assume a prior distribution $\pi(\cdot)$, which is a probability measure with respect to the measurable space $(\Theta, \sigma(\Theta))$. Upon observing a realization y^T of the sequence Y^T , we define the prequential posterior (PP) as,

$$\pi_P(\theta \mid y^T) \propto \pi(\theta) \exp(-\gamma L_T(\theta)), \quad (1)$$

where γ is a free parameter which controls how much the cumulative loss influences the posterior relative to the prior distribution. By taking $\gamma = 1$ and the loss function to be the negative log likelihood function of a timeseries model with known likelihood functions, we recover the standard Bayesian posterior distribution for the timeseries model from the prequential posterior.

2.2 Consistency of the prequential posteriors

Before delving into the asymptotic properties of the prequential score and the posterior it induces, let us first consider the case where the observations are assumed to be IID and suppose the model likelihood is known. The uniform law of large numbers (ULLN) leads to the asymptotic consistency of the maximum likelihood estimator to the true parameter (θ^*) .

However, this classical result breaks down when strong dependence exists between successive observations. In such cases, the ULLN does not apply naturally. The consistency of extremum estimators, those that minimize the prequential loss, has instead been established under asymptotic mixing conditions on the data-generating process. Loosely speaking, these conditions imply that as $m \rightarrow \infty$, Y_{t-m} and Y_t become independent (Pacchiardi et al., 2024a). This covers settings such as fixed-order Markov processes, but does not extend to models with strong or long-range temporal dependencies.

Nevertheless, a fundamental challenge arises when the true data-generating process does not lie within the assumed model class: how should we define consistency in such cases? To illustrate this, we draw on an example from Skouras and Dawid (2000), which highlights the need for an alternative notion of consistency.

Example from Skouras and Dawid (2000) Suppose that (X_t) is a sequence of IID random variables distributed as $\mathcal{N}(0, 1)$. Define the observed process as $Y_t = X_0 + X_t$. Consider a model $\mathbb{E}_{t-1}(Y_t) = \theta$ for some constant θ . We estimate θ by minimizing the

squared error loss:

$$\bar{L}_T(\theta) = \frac{1}{T} \sum_{t=1}^T (Y_t - \theta)^2,$$

whose minimizer is

$$\hat{\theta}_T = \arg \min_{\theta} L_T(\theta) = \frac{1}{T} \sum_{t=1}^T Y_t.$$

However, the expected loss is given by:

$$\bar{L}_T^{**}(\theta) = \mathbb{E} \bar{L}_T(\theta) = \frac{1}{T} \sum_{t=1}^T \mathbb{E}(Y_t - \theta)^2 = \mathbb{E}(Y_t^2) + \theta^2 = 2 + \theta^2,$$

which is minimized at $\theta^{**} = 0$. On the other hand, we note that $\hat{\theta}_T = X_0 + \frac{1}{T} \sum_{t=1}^T X_t$, which converges almost surely to the observed value x_0 of X_0 as $T \rightarrow \infty$. Therefore, $\hat{\theta}_T \not\rightarrow \theta^{**}$, but instead converges to a data-dependent limit.

These limitations motivate us to explore an alternative framework for analyzing the consistency of prequential loss minimizers introduced in Skouras and Dawid (2000) and Dawid and Tewari (2020). Note that both the true observation Y_t and the prediction of the model \hat{Y}_t at time t depend on previous observations $Y_{1:t-1}$. As a result, different histories of $Y_{1:t-1}$ can yield different conditional distributions for Y_t . In the case of non-ergodic models, this dependence on past observations may persist indefinitely. Therefore, it is more appropriate to assess predictive performance using conditional expectations rather than marginal ones. Hence, we define the conditional predictive risk as the conditional expected loss at time t given by:

$$\ell_t^*(\theta) = \mathbb{E}_{t-1}[\ell_t(\theta)],$$

where $\mathbb{E}_{t-1}(\cdot) = \mathbb{E}(\cdot \mid \mathcal{F}_{t-1})$ denotes the conditional expectation given the filtration \mathcal{F}_{t-1} , i.e., all observations up to time $t-1$.

The conditionally expected score $\ell_t^*(\theta)$ thus captures the one-step ahead predictive risk of the model, given the observed history up to time $t-1$. We denote the expected prequential loss by,

$$L_T^*(\theta) = \sum_{t=1}^T \mathbb{E}_{t-1}[\ell_t(\theta)].$$

Returning to the example from Skouras and Dawid (2000), we can define the one-step-ahead predictive risk as

$$\bar{L}_T^*(\theta) = \frac{1}{T} \sum_{t=1}^T \mathbb{E}_{t-1}(Y_t - \theta)^2 = \frac{1}{T} \sum_{t=1}^T \mathbb{E}_{t-1}(X_0 + X_t - \theta)^2 = (X_0 - \theta)^2 + 1.$$

This conditional risk is minimized at $\theta_T^* = X_0$. Since the extremum estimator is given by $\hat{\theta}_T = \frac{1}{T} \sum_{t=1}^T Y_t = X_0 + \frac{1}{T} \sum_{t=1}^T X_t$, we also have that $|\hat{\theta}_T - \theta_T^*| \rightarrow 0$ almost surely as $T \rightarrow \infty$.

This illustrates that the minimizer of the empirical prequential loss is a consistent estimator of θ_T^* , which minimizes the conditional predictive risk, instead of the expected risk.

When the true data-generating process does not lie within the assumed model class, it is not meaningful to speak of a ‘true parameter’ that generated the observations. In such settings, where models are viewed as predictive systems rather than data-generating mechanisms, consistency should instead be defined in terms of the ability to select a predictor that minimizes the conditional predictive risk. This is the interpretation of this alternative consistency, first proposed in Skouras and Dawid (2000) for misspecified models.

Moreover, this predictive notion of consistency extends naturally to non-stationary and non-ergodic settings, as shown in Example 4 of Skouras (1998). The authors also emphasize that the choice of loss function plays a critical role: different loss functions may yield different approximations to the true data-generating process (see Example 5 in Skouras (1998)). Thus, the choice of the loss function should be guided by the goals of the specific inferential task at hand.

Next, we formally present a ULLN for martingales proved in Skouras and Dawid (2000) under the following conditions.

A1 The metric space (Θ, d) is compact.

A2 With P probability 1, there exists an $A_t < \infty$ for all $t = 1, 2, \dots$ such that one of the following conditions hold,

(a)

$$\sum_{t=1}^{\infty} \frac{\mathbb{E}_{t-1} \left\{ \sup_{\theta \in \Theta} |\ell_t(\theta)|^2 \right\}}{A_t} < \infty; \text{ or,}$$

(b) there exists an $\epsilon > 0$ such that

$$\left(\sum_{t=1}^T \mathbb{E}_{t-1} \left\{ \sup_{\theta \in \Theta} |\ell_t(\theta)|^2 \right\} \right)^{(1+\epsilon)/2} = \mathcal{O}(A_T).$$

A3 For each $\theta \in \Theta$, there is a constant $\tau > 0$, such that for every $s, d(\theta, s) \leq \tau$ implies that for every $t \geq 1$, P -a.s.,

$$|\ell_t(\theta) - \ell_t(s)| \leq B_t(Y_t) h\{d(\theta, s)\}$$

where $\{B_t(\cdot)\}$ is a sequence of \mathcal{F}_t -measurable functions such that P -a.s.,

$$\limsup_T \frac{1}{A_T} \sum_{t=1}^T \mathbb{E}_{t-1} \{B_t(Y_t)\} < \infty$$

and $h(\cdot)$ is a non-random function such that $h(y) \downarrow h(0) = 0$ as $y \downarrow 0$. The null sets, $B_t(\cdot)$ and h may depend on θ .

Remark 1 It is always possible to find an A_T that satisfies the assumption **A2**. Clearly, assumptions **A2** and **A3** are stronger than those required in the IID setting, where it suffices to assume that the loss is dominated by an integrable function. However, these conditions help control the stochastic behavior and continuity of the empirical prequential loss.

Remark 2 As discussed earlier, Pacchiardi et al. (2024a) established consistency of the empirical prequential risk minimizer under asymptotic stationarity, certain mixing conditions that guarantee vanishing dependence between distant observations, and moment boundedness of the loss function. In that sense, assumption **A2** can be viewed as analogous to the moment boundedness condition in Pacchiardi et al. (2024a). This regularity allows our results to extend to settings with stronger temporal dependencies, without requiring either asymptotic stationarity or any form of mixing assumptions.

With a normalizing constant A_T that satisfies the assumption **A2**, next we define the normalized prequential loss as,

$$\bar{L}_T(\theta) = \frac{1}{A_T} \sum_{t=1}^T \ell_t(\theta),$$

and the normalized expected prequential loss as,

$$\bar{L}_T^*(\theta) = \frac{1}{A_T} \sum_{t=1}^T \mathbb{E}_{t-1}[\ell_t(\theta)].$$

Note that A_T is taken as T in the example previously discussed from Skouras and Dawid (2000). Next, we state the ULLN for martingales.

Lemma 3 Under assumptions **A1-A3**, a uniform law of large numbers (ULLN) for martingales holds, which implies, with probability one under P ,

$$\sup_{\theta \in \Theta} |\bar{L}_T(\theta) - \bar{L}_T^*(\theta)| \rightarrow 0.$$

Note that Skouras and Dawid (2000) originally proved the above lemma under a different set of assumptions. However, they later introduced assumptions **A2** and **A3** as alternative conditions that are easier to verify in practice. For completeness, we include the original assumptions along with the full lemma statement in Appendix A.1. Next, we assume that the expected prequential score converges to a finite limit.

A4 There exists a function $\bar{L}^*(\theta)$ such that as $T \rightarrow \infty$, $\bar{L}_T^*(\theta) \rightarrow \bar{L}^*(\theta)$ uniformly with probability one under P .

Corollary 4 Under the assumptions **A1-A4**, it follows from Lemma 3 that,

$$\sup_{\theta \in \Theta} |\bar{L}_T(\theta) - \bar{L}^*(\theta)| \rightarrow 0 \text{ as } T \rightarrow \infty,$$

with probability one under P .

The above lemma is a direct consequence of Lemma 3 and assumption **A4**. A short proof can be found in Appendix A.2. We will use this result in addition to the following assumptions to establish a Bernstein-von Mises type theorem on the asymptotic behaviour of the generalized posterior.

A5 The metric space (Θ, d) is separable.

A6 For every t and each $\theta \in \Theta$, the functions $\ell_t(\theta)$ is \mathcal{F}_t measurable, and continuous on Θ almost surely, *i.e.* it is continuous for all ω in an event $F_t \in \mathcal{F}_t$ such that $P(F_t) = 1$.

Remark 5 When the assumptions **A1**, **A5** and **A6** hold, then it follows from the following general lemma (Gallant and White, 1988; White, 1996) that $\bar{L}_T(\theta)$ admits a measurable minimizer. We denote this minimizer by,

$$\hat{\theta}_T = \arg \min_{\theta \in \Theta} \bar{L}_T(\theta).$$

We provide the complete statement of the lemma on the existence of the extremum estimator in Appendix A.3.

Next, we establish the consistency of the sequence of estimators given by $\{\hat{\theta}_T\}_{T=1}^{\infty}$ to θ^* defined below.

A7 The function $\bar{L}^*(\theta)$ has a minimum, P -a.s. on Θ at θ^* . Let $\epsilon > 0$ and $B^c(\epsilon) = \{\theta \in \Theta : d(\theta, \theta^*) \geq \epsilon\}$. Then P -a.s.

$$\min_{\theta \in B_T^c(\epsilon)} \bar{L}^*(\theta) - \bar{L}^*(\theta^*) > 0.$$

Lemma 6 Suppose that assumptions **A1-A7** hold, then

$$d(\hat{\theta}_T, \theta^*) \rightarrow 0,$$

with probability one under P .

We derive the above lemma using a result from Skouras (1998) and a detailed proof can be found in Appendix A.4.

Remark 7 For Lemma 6 to hold, the parameter space needs to be compact and the empirical prequential score must be smooth enough in the neighbourhood of θ^* as in condition **A5**. Then, this result is analogous to the consistency of maximum likelihood estimators (MLE). Specifically, when the loss function is the negative loglikelihood, the estimator $\hat{\theta}_T$ is the MLE. The result establishes that $\hat{\theta}_T$ is consistent for θ^* , the true parameter under a well-specified model, *i.e.*, when $P = Q^{\theta^*}$. In the misspecified case, where $P \notin \mathcal{Q}$, the parameter θ^* corresponds to the model within \mathcal{Q} that minimizes the expected prequential loss, *i.e.*, the model with optimal one-step-ahead predictive performance.

Using these consistent estimators of θ^* , we next state the BvM theorem for the generalized prequential posterior under the following assumptions.

A8 $\pi : \mathbb{R}^p \rightarrow \mathbb{R}$ is a probability distribution with respect to the Lebesgue measure such that π is continuous at θ^* and $\pi(\theta^*) > 0$.

A9 $\bar{L}_T(\theta)$ have continuous third derivatives in E and the third derivatives $\bar{L}_T'''(\theta)$ are uniformly bounded in E .

A10 $\bar{L}_T''(\theta^*) \rightarrow H^*$ as $T \rightarrow \infty$ for some positive definite H^* .

A11 $\theta^*, \hat{\theta}_T \in E$ for sufficiently large T , where $E \subseteq \mathbb{R}^p$ is open and convex.

A12 For any $\epsilon > 0$, $\liminf_T \inf_{\theta \in B_\epsilon^c(\hat{\theta}_T)} (\bar{L}_T(\theta) - \bar{L}_T(\hat{\theta}_T)) > 0$.

Theorem 8 Suppose the assumptions **A1-A12** hold. Then, there exists a sequence of estimators $\{\hat{\theta}_T\}_{T=1}^\infty$ such that as $T \rightarrow \infty$, with probability one under P , $\hat{\theta}_T \rightarrow \theta^*$.

On defining $z_T = \int_{\Theta} \exp(-L_T(\theta)) \pi(\theta) d\theta$ and $\pi_P(\theta|y^T) = \pi(\theta) \exp(-L_T(\theta))/z_T$ ¹ we have,

$$\int_{B_\epsilon(\theta^*)} \pi_P(\theta|y^T) d\theta \xrightarrow{T \rightarrow \infty} 1 \quad \text{for all } \epsilon > 0, \quad (2)$$

which means, $\pi_P(\theta|y^T)$ concentrates at θ^* ;

$$z_T \approx \frac{\exp(-L_T(\hat{\theta}_T)) \pi(\theta^*)}{|\det H^*|^{1/2}} \left(\frac{2\pi}{A_T} \right)^{p/2} \quad (3)$$

as $T \rightarrow \infty$ (Laplace approximation), and letting q_T be the density of $\sqrt{A_T}(\theta - \hat{\theta}_T)$ when $\theta \sim \pi_P(\theta|y^T)$,

$$\int_{\Theta} |q_T(\theta) - \mathcal{N}(\theta | \mathbf{0}, H^{*-1})| d\theta \xrightarrow{T \rightarrow \infty} 0, \quad (4)$$

which implies, q_T converges to $\mathcal{N}(\mathbf{0}, H^{*-1})$ in total variation.

We prove the above BvM theorem using two results from Miller (2021), and we provide a sketch of the proof in Appendix A.5. The theorem states that as more data is observed, the prequential posterior concentrates around the θ^* . It also begins to resemble a Gaussian distribution. The covariance matrix of this Gaussian is given by the inverse of H^* , which plays the role of the Fisher information matrix in the likelihood-based framework.

2.3 Prequential scoring rule posterior

Previously, we discussed how a discrepancy measure between forecasts from a simulator model and actual observations can define a generalized posterior in the absence of a tractable likelihood function. In this section, we consider scoring rules as a principled way to define such loss functions.

Scoring rules The scoring rules (SR) originate from the framework of probabilistic forecasting (Winkler, 1967; Murphy and Winkler, 1970; Savage, 1971; Matheson and Winkler, 1976), where the objective is to quantify the uncertainty associated with a forecast. They are widely used to assess the quality and calibration of probabilistic predictions. An SR $S(Q, y)$ assigns a penalty to a probabilistic model Q when y is observed as a realization of the random variable Y . Intuitively, if the model Q is close to the true underlying process, it incurs a smaller penalty, and vice versa.

1. From this point onward, we set $\gamma = 1$ in equation (1) wherever the generalized posterior is defined. However, other values of γ can be absorbed into the loss function without loss of generality.

Let P denote the true data-generating process, i.e., $Y \sim P$. Then, the expected score under P is defined as:

$$\tilde{S}(Q, P) = \mathbb{E}_{Y \sim P}[S(Q, Y)].$$

A scoring rule is said to be *proper* if this expected score is minimized when $Q = P$, and *strictly proper* if the minimum is uniquely achieved at $Q = P$.

This definition of the properness of scoring rules can be interpreted using the idea of a statistical divergence. Let us define $D(Q, P) = \tilde{S}(Q, P) - \tilde{S}(P, P)$. S is said to be proper if $D(Q, P)$ is a statistical divergence between two probability distributions Q and P . This means that $D(P, Q) \geq 0$ for any probability distributions P, Q . Further, $P = Q$ implies $D(Q, P) = 0$ but the converse only holds when S is strictly proper. This implies that if the true model P is well specified by some model class \mathcal{Q} and the associated scoring rule is proper, then by minimizing the expected scoring rule, one can recover the true model by some $Q^* \in \mathcal{Q}$ where $Q^* = \arg \min_{Q \in \mathcal{Q}} D(Q, P) = \arg \min_{Q \in \mathcal{Q}} \tilde{S}(Q, P)$. Further, P is the only solution of Q^* , if the scoring rule is strictly proper.

Some examples of scoring rules are the continuous ranked probability score (CRPS) (Székely and Rizzo, 2005), energy score or kernel score (Gneiting and Raftery, 2007) etc. For later sections, we will be using the energy score, which is a multivariate generalization of CRPS, defined as,

$$S_E^{(\beta)}(Q, \mathbf{y}) = 2 \cdot \mathbb{E} \|X - \mathbf{y}\|_2^\beta - \mathbb{E} \|X - X'\|_2^\beta, \quad X, X' \sim Q; \quad \beta \in (0, 2). \quad (5)$$

This is a strictly proper scoring rule for the class of probability measures $\mathcal{Q} = \{Q : \mathbb{E}_{X \sim Q} \|X\|^\beta < \infty, \forall \beta \in (0, 2)\}$ (Gneiting and Raftery, 2007). The related divergence is the square of the energy distance, which is a metric between probability distributions. Further the energy score can be unbiasedly estimated using $\mathbf{x}_j \sim Q, j = 1, \dots, m$ which are independent and identically distributed samples from the model Q , and the estimate is given by,

$$\hat{S}_E^{(\beta)} \left(\{\mathbf{x}_j\}_{j=1}^m, \mathbf{y} \right) = \frac{2}{m} \sum_{j=1}^m \|\mathbf{x}_j - \mathbf{y}\|_2^\beta - \frac{1}{m(m-1)} \sum_{\substack{j, k=1 \\ k \neq j}}^m \|\mathbf{x}_j - \mathbf{x}_k\|_2^\beta, \quad \beta \in (0, 2). \quad (6)$$

For our implementation, we will consider $\beta = 1$ and will write $S_E^{(1)}(P, \mathbf{y})$ simply as $S_E(P, \mathbf{y})$.

Prequential scoring rule The scoring rule-based framework can be extended to handle temporal data as done by Pacchiardi et al. (2024a). Suppose our simulator model at time t , denoted by Q_t^θ , approximates the conditional distribution of Y_t given its past values, $Y_{1:t-1}$. Then, using a scoring rule S , we define the loss as $\ell_t(\theta) = S(Q_t^\theta, Y_t)$.

Upon observing the time series $Y^T = (Y_1, Y_2, \dots, Y_T)$, the prequential score is given by,

$$L_T(\theta) = \sum_{t=1}^T S(Q_t^\theta, Y_t). \quad (7)$$

$L_T(\theta)$ evaluates the performance of the sequence of one step ahead predictions produced by the model Q^θ given the observed history. Consequently, from equation (1), we define

the generalized prequential scoring rule posterior as,

$$\pi_{PSR}(\theta \mid y^T) \propto \pi(\theta) \exp(-L_T(\theta)) = \pi(\theta) \exp\left(-\sum_{t=1}^T S(Q_t^\theta, y_t)\right). \quad (8)$$

3 Sequential inference of prequential posteriors

In this section, we describe our sampling strategy for a high-dimensional parameter space (with dimension ~ 1000) to sample from the prequential posterior distribution defined previously. First, we define an episode of length τ as $Y_{\tau(i-1)+1:\tau i}$, where $i = 1, 2, \dots$. These episodes can be viewed as an update schedule, since it is often undesirable to update model parameters upon the arrival of every single datapoint. Instead, we choose an update schedule based on a fixed episode length, after which we recompute the posterior distribution. With a slight abuse of notation, we write the posterior distribution of the model parameters after observing $Y^{\tau t}$ as

$$\pi_t(\cdot) = \pi_{PSR}(\cdot \mid y^{\tau t}).$$

This defines a sequence of target distributions from which we want to sample. The sequence is given by $\{\pi_1(\cdot), \pi_2(\cdot), \dots\}$, corresponding to the posterior distributions after observing the data series $Y^\tau, Y^{2\tau}, \dots$. To sample from this sequence, we propose the use of Sequential Monte Carlo (SMC) samplers (Del Moral et al., 2006).

3.1 Sequential Monte Carlo

SMC provides a powerful class of sampling algorithms that originated from particle filters used in state-space models. These samplers have since been extended to a wide range of statistical problems involving complex target distributions. The key idea is to use a set of particles and propagate them through the sequence of target distributions starting from a proposal distribution. Traditional sampling methods, such as importance sampling and Markov chain Monte Carlo (MCMC), are well-established but may face limitations in high-dimensional or dynamic settings. SMC samplers integrate the strengths of both these methods in a way that enhances its scalability.

In practice, SMC approximates the sequence of target distributions using a population of particles that evolve through a combination of MCMC moves, importance sampling, and resampling to avoid degeneracy. Let us consider the Markov kernel $M_t(\theta_{t-1}, d\theta_t)$ such that it is π_{t-1} invariant which means, $\pi_{t-1} M_t = \pi_{t-1}$ for $t \geq 1$, where we use the notation θ_t to denote a particle at t -th iteration of SMC. We can then define the following sequence of Feynman-Kac distributions for $t = 0, 1, 2, \dots$ as,

$$\mathbb{F}_t(d\theta_{0:t}) = \frac{1}{z_t} \pi(d\theta_0) \prod_{s=1}^t M_s(\theta_{s-1}, d\theta_s) \prod_{s=0}^t G_s(\theta_s). \quad (9)$$

Here, the potential function is given by $G_s(\theta) = L_{s\tau}(\theta)/L_{s(\tau-1)}(\theta) = \sum_{t=s(\tau-1)+1}^{s\tau} l_t(\theta)$. The construction above ensures that the marginal distribution of θ_t (with respect to \mathbb{F}_t) is π_t . We use this formulation to set up an SMC sampler with MCMC moves, following the approach suggested in Del Moral et al. (2006)[Section 3.3.2.3]. In practice, however, it is

often challenging to employ an exact MCMC kernel with the correct invariant distribution, since the Metropolis correction step is frequently omitted to reduce computational cost. The details of our Markov kernel implemented are provided in Section 3.4.

3.2 Adaptive tempering within SMC

It is important for the efficiency of SMC samplers that the proposal and target distributions are sufficiently close to avoid weight degeneracy. To address this, we utilize an adaptive strategy based on the *conditional effective sample size* (CESS) (Zhou et al., 2016), which automatically determines the sequence of intermediate distributions to ensure smooth propagation of particles within each episodic update. Intuitively, CESS quantifies the overlap between two successive distributions, which can be evaluated using the incremental weights corresponding to a hypothetical transition between these distributions.

In our framework, since the incremental weight can be computed prior to the forward propagation of particles, we enforce a constant overlap across successive intermediate distributions by keeping the CESS fixed. This avoids degeneracy during weight computation. To transition particles from $\pi_{t-1}(\cdot)$ to $\pi_t(\cdot)$, we define a sequence of intermediate distributions as:

$$\left\{ \pi_t^{(l)}(\theta) = \pi_{t-1}(\theta)^{1-\alpha_l} \pi_t(\theta)^{\alpha_l} \right\}_{l=1}^L,$$

where the *temperatures* $\{\alpha_l\}$ are such that $0 < \alpha_1 < \alpha_2 < \dots < \alpha_L = 1$. These temperature values are adaptively chosen so that the CESS remains constant across transitions, thereby ensuring a smooth evolution of the particle system through the episodic posterior updates.

3.3 Wastefree SMC

We previously discussed how SMC samplers employ forward kernels to propagate particles from a proposal distribution towards the target distribution. In high-dimensional settings, it is critical that these kernels exhibit strong mixing properties to ensure adequate exploration of the sample space. In practice, when sampling from a high-dimensional parameter space, it is common to apply multiple iterations of MCMC moves to reduce the variance. However, only the final sample in the chain is typically retained as the next particle, while the intermediate samples are discarded. This seems like a loss of potentially valuable computational effort.

Dau and Chopin (2022) proposed a strategy to mitigate this inefficiency by utilizing *all* intermediate samples generated by the MCMC chains. This approach enables a larger effective number of particles to represent the target distribution, without incurring a prohibitive increase in computational cost.

The key idea is as follows: suppose that we aim to generate N particles to represent the posterior distribution at each update step. Instead of sampling all N particles independently, we first resample $M \ll N$ particles from the current population. From each of these M particles, we initiate an MCMC chain of length P , resulting in a total of $N = MP$ particles when all chain samples are collected. This strategy is particularly advantageous in parallel computing environments where each of the M MCMC chains can be executed simultaneously on M cores. This offers a computationally efficient means of generating a diverse particle population.

Furthermore, the authors provide a Feynman–Kac model interpretation of the *waste-free* SMC algorithm. The fundamental difference from standard SMC lies in the structure of the target space: rather than sampling in Θ , the algorithm samples paths in the extended space Θ^P , with each path corresponding to a full MCMC trajectory of length P . They exploit this duality to establish theoretical guarantees, including the consistency and asymptotic normality of the particle approximation.

3.4 Preconditioned Forward Kernel

Efficient sampling becomes increasingly challenging as the dimensionality of the parameter space grows, a phenomenon commonly referred to as the *curse of dimensionality*. This issue affects most sampling methods, including SMC, MCMC, and their variants. To address this, gradient-based Markov kernels (Welling and Teh, 2011; Chen et al., 2014; Ding et al., 2014) are often employed to enhance exploration of the parameter space by leveraging gradient information.

One widely used gradient-based approach is *stochastic gradient Langevin dynamics* (SGLD) (Welling and Teh, 2011), which generates samples by discretizing a stochastic differential equation (SDE). The Euler–Maruyama scheme is typically used for discretization due to its simplicity, although it introduces discretization bias. Further, to mitigate the effect of noisy gradient estimates, momentum and friction terms can be incorporated, leading to the *stochastic gradient Nosé–Hoover thermostat* (SGNHT) algorithm (Leimkuhler and Shang, 2016). This method operates in an extended state space that includes both parameters and auxiliary momentum variables, and has found successful application in Bayesian inference (Ding et al., 2014; Pacchiardi et al., 2024b; Roy et al., 2024).

Additionally, preconditioning strategies have been proposed to further improve sampling efficiency in high-dimensional spaces. For example, Girolami and Calderhead (2011) introduced Riemannian geometry-based preconditioning, while Chen et al. (2016) proposed using the squared gradient of the loss, akin to the preconditioners used in adaptive optimizers like RMSprop and Adam. We adopt the latter approach in our work. Furthermore, to improve numerical accuracy when solving the SDE, we use a symmetric splitting scheme (as shown in Chen et al. (2016)), which provides better approximation quality at the cost of slightly increased computation.

The following pseudo-algorithm outlines our forward Markov kernel for sampling from a distribution with density proportional to $\pi(\theta) \cdot \exp\{-L_T(\theta)\}$, where $L_T(\theta)$ denotes the (prequential) loss and $\pi(\theta)$ is the prior. The corresponding potential function is defined as

$$U(\theta) = L_T(\theta) - \log \pi(\theta).$$

Our method is inspired by the Santa-SSS algorithm introduced in Chen et al. (2016).

Algorithm 1: Preconditioned forward kernel

Input: Learning rate η , parameters σ, λ , noise $\{\zeta_t \sim \mathcal{N}(\mathbf{0}, \mathbf{I}_p)\}$

Initialize: $\theta_0, \mathbf{u}_0 = \sqrt{\eta} \cdot \mathcal{N}(0, \mathbf{I}_p)$, $\boldsymbol{\alpha}_0 = \sqrt{\eta} \cdot C$, $\mathbf{v}_0 = \mathbf{0}$

for $n = 1, 2, \dots$ **do**

Compute stochastic gradient: $\tilde{\mathbf{f}}_n \leftarrow \nabla_{\theta} \tilde{U}(\theta_{n-1})$;
 $\mathbf{v}_n \leftarrow \sigma \mathbf{v}_{n-1} + \frac{1-\sigma}{T^2} \tilde{\mathbf{f}}_n \odot \tilde{\mathbf{f}}_n$;
 $\mathbf{g}_n \leftarrow 1 \oslash \sqrt{\lambda + \sqrt{\mathbf{v}_n}}$;
 $\theta_n \leftarrow \theta_{n-1} + \frac{1}{2} \mathbf{g}_n \odot \mathbf{u}_{n-1}$;
 $\boldsymbol{\alpha}_n \leftarrow \boldsymbol{\alpha}_{n-1} + \frac{1}{2} (\mathbf{u}_{n-1} \odot \mathbf{u}_{n-1} - \eta)$;
 $\mathbf{u}_n \leftarrow \exp(-\boldsymbol{\alpha}_n/2) \odot \mathbf{u}_{n-1}$;
 $\mathbf{u}_n \leftarrow \mathbf{u}_n - \eta \cdot \mathbf{g}_n \odot \tilde{\mathbf{f}}_n + \sqrt{2 \cdot \mathbf{g}_{n-1} \eta^{3/2}} \odot \zeta_n$;
 $\mathbf{u}_n \leftarrow \exp(-\boldsymbol{\alpha}_n/2) \odot \mathbf{u}_n$;
 $\boldsymbol{\alpha}_n \leftarrow \boldsymbol{\alpha}_n + \frac{1}{2} (\mathbf{u}_n \odot \mathbf{u}_n - \eta)$;
 $\theta_n \leftarrow \theta_n + \frac{1}{2} \mathbf{g}_n \odot \mathbf{u}_n$;

end

We employ the above Markov kernel in Algorithm 1 within the waste-free SMC framework. Note that we do not use a Metropolis accept–reject step; instead, the next particle is always accepted. While this introduces an approximation error, it reduces computational overhead.

Moreover, to obtain an unbiased estimate of the prequential loss $L_T(\theta)$, consider an alternative representation of the energy score:

$$\ell_t(\theta) = S(Q_t^\theta, Y_t) = \mathbb{E}_{X, X' \sim Q_t^\theta} g(X, X', Y_t),$$

for some function g . Q_t^θ being a DGFM, a simulation from the model can be expressed as $X = h_\theta(W_1)$, where the function h_θ is defined by deep neural networks parameterized by θ and W_1 is drawn from an auxiliary distribution W , independent of θ , as shown in Pacchiardi et al. (2024b). Under mild regularity conditions, and assuming both h_θ and g are differentiable with respect to θ , we can interchange expectation and differentiation, yielding:

$$\begin{aligned} \nabla_\theta S(Q_t^\theta, Y_t) &= \nabla_\theta \mathbb{E}_{X, X' \sim Q_t^\theta} g(X, X', Y_t) \\ &= \nabla_\theta \mathbb{E}_{W_1, W_2 \sim W} g(h_\theta(W_1), h_\theta(W_2), Y_t) \\ &= \mathbb{E}_{W_1, W_2 \sim W} \nabla_\theta g(h_\theta(W_1), h_\theta(W_2), Y_t), \end{aligned}$$

where the gradient can be calculated using automatic-differentiation. This explains how we unbiasedly estimate the score using independent draws from the base distribution W . In the next section, we illustrate the application of this algorithm with two examples.

4 Prequential posteriors in practice

We demonstrate our data assimilation strategy using the generalized prequential posterior on two datasets: a time series model for weather forecasting introduced in Lorenz (1996), and an open-source meteorological benchmarking dataset called *WeatherBench*. For Lorenz 96, we also compare our method with the ensemble Kalman filter, assuming a commonly

used but misspecified state-space model. In both of our examples, we employ a deep generative forecasting model as the simulator. As the true likelihood function is intractable for such models, we instead define the prequential posterior using energy score as the loss function. Specifically, we use the energy score (Equation 5), and obtain an unbiased estimate of the prequential score via the Monte Carlo approximation in Equation 6, applied to the prequential form given in Equation 7.

To incorporate new data sequentially, we partition the training data into fixed-length episodes of size τ ; where we have taken $\tau = 100$ for Lorenz 96 and $\tau = 362$ (~ 1 year) for WeatherBench. The generalized posterior is updated at the end of each episode using an SMC sampler. The proposal distribution is taken to be a multivariate standard Gaussian, though we also examined the effect of alternative choices (e.g., Student's t-distribution), with results presented in the Appendix B.1. In all cases, the prior is chosen to be identical to the proposal. The tempering of the episodic posteriors is performed by keeping the conditional effective sample size (CESS) fixed to a threshold, ensuring adaptive yet stable intermediate distributions. Full implementation details are provided in the Appendix B.2.

We assess the predictive performance of the episodic SMC samples on a held-out test dataset. For each episodic posterior, we evaluate the quality of the probabilistic forecasts using a probabilistic calibration metric (*calibration error*) and two deterministic metrics: the *normalized root mean squared error* (NRMSE) and the *coefficient of determination* (R^2). A detailed description of these metrics is provided in Appendix B.3.

4.1 Lorenz 96

The Lorenz96 model (Lorenz, 1996) is a simplified, yet widely used system designed to mimic key features of atmospheric dynamics. It consists of two types of variables: slow-evolving variables y and fast-evolving variables x and we only record the slow-evolving y variable as observations. The coupled evolution of these variables is governed by the following set of nonlinear differential equations:

$$\begin{aligned}\dot{y}(k) &= -y(k-1) \left(y(k-2) - y(k+1) \right) - y(k) + F - \frac{hc}{b} \sum_{j=J(k-1)+1}^{kJ} x(j) \\ \dot{x}(j) &= -cbx(j+1) \left(x(j+2) - x(j-1) \right) - cx(j) + \frac{hc}{b} Y_{\lfloor (j-1)/J \rfloor + 1}\end{aligned}\quad (10)$$

where $y(k)$ and $x(j)$ denote the k th and the j th component of the respective variables. Here, $k = 1, \dots, K$ and $j = 1, \dots, JK$, with cyclic boundary conditions applied such that $k = K + 1$ maps to $k = 1$, and similarly for j . These equations capture the interactions between slow and fast variables in a structured, recurrent fashion—each y is influenced by a group of J fast components x .

Following the experimental setup in Pacchiardi et al. (2024a), we fix the model parameters to $K = 8$, $J = 32$, $h = 1$, $b = 10$, $c = 10$, and $F = 20$. We integrate the system using the fourth-order Runge–Kutta (RK4) method with a discretization step of $dt = 0.001$. The initial conditions are set to $y(1) = x(1) = 1$, while all other components are initialized to zero. After discarding the first 2 units of simulated time (to allow transients to settle), the values of y are recorded every $\Delta t = 0.2$, roughly corresponding to one atmospheric day in

terms of predictive dynamics. Simulation is carried out for 4000 additional time units. The resulting dataset is divided into training and test portions using an 80% – 20% split.

The deep generative forecasting model (DGF) We define our model class \mathcal{Q} as a family of generative models with a Markov dependency structure of order 10. This implies that the prediction at time t depends on the preceding 10 observations.

The generative model architecture takes an input sequence $Y_{t-k:t-1}$, which is fed into a single-layer gated recurrent unit (GRU) network with a hidden size of 16. The output from the GRU is concatenated with a latent noise vector $W \sim \mathcal{N}(0, 1)$, where $W \in \mathbb{R}^1$. This combined feature representation is then passed through a stack of three fully connected (dense) layers, which outputs the prediction for the next time step Y_t , for $t = k+1, k+2, \dots$. The total number of trainable parameters in this simulator amounts to $p = 4442$.

Ensemble Kalman filter with a misspecified state-space model To benchmark our method against a standard baseline, we employ the ensemble Kalman filter (EnKF). The following state-space model is commonly used for inference in the Lorenz–96 system (see, for example, Roth et al. (2017) and Duran-Martin et al. (2024)), where x denotes the latent state and y the noisy observation:

$$\begin{aligned}\dot{x}(k) &= (x(k+1) - x(k-2))x(k-1) - x(k) + F_k, \\ y(k) &= x(k) + \psi_k,\end{aligned}\tag{11}$$

with $F_k \sim \mathcal{N}(20, 1)$ and $\psi_k \sim \mathcal{N}(0, 1)$ for $k = 1, 2, \dots, K$, where $K = 8$. Note that this simplified model is obtained by isolating the slow-variable equation from (10) and treating the forcing term F as known, following Lorenz (1996). Nevertheless, the model remains misspecified relative to the full system, since the assumed Gaussian observation noise cannot capture the chaotic variability introduced by the fast variables. We then discretize (11) using a fourth-order Runge–Kutta (RK4) method, yielding the nonlinear state transition equations employed by the EnKF.

Empirical findings We infer the prequential posterior after each episode and assess its predictive performance on a separate dataset using calibration error, NRMSE, and R^2 . In the top panel of Figure 2, we evaluate the predictive accuracy of the posterior obtained after the i th episode on the data segment $(\tau i + 1, (\tau + 1)i)$ for $i = 1, \dots, 100$. For comparison, the EnKF continually updates its predictive distribution at every time step, and we compute the same diagnostic metrics. Because the state-space model assumed by the EnKF is misspecified, its predictive accuracy does not improve even as more data are observed. In contrast, our method progressively learns a model that better represents the underlying data-generating mechanism, leading to substantial improvement in predictive accuracy: although initially poor, it eventually surpasses the performance of the EnKF.

In the bottom panel of Figure 2, the diagnostic metrics are evaluated on a separate test set of length 2000. As additional episodes are incorporated, both the calibration error and the normalized RMSE decrease and approach zero, indicating enhanced calibration and accuracy. Simultaneously, the coefficient of determination R^2 increases towards 1, which aligns with the theoretical result according to Theorem 8 on posterior consistency.

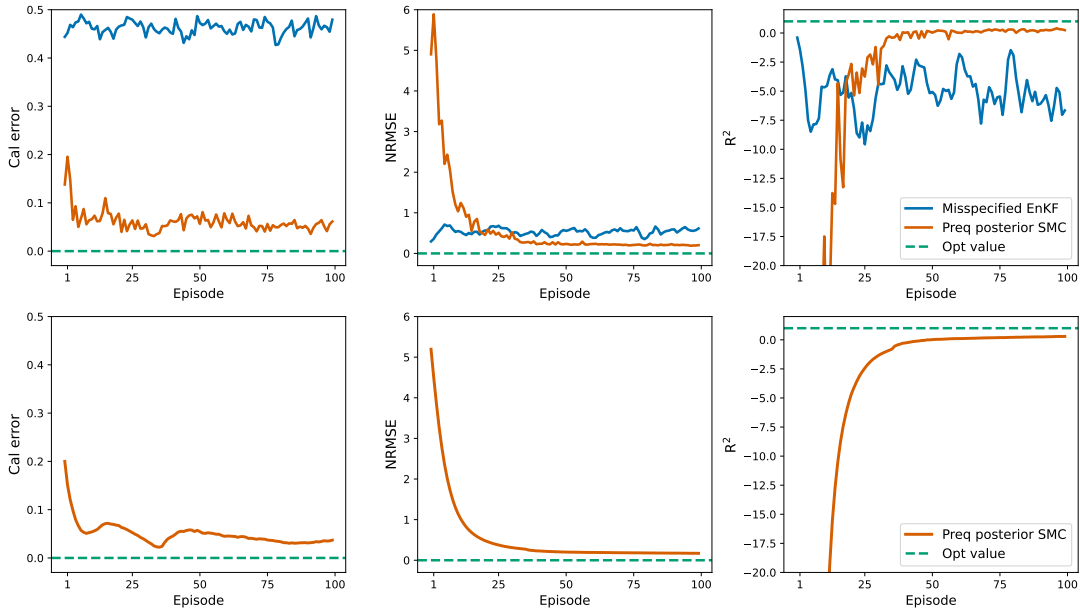


Figure 2: Posterior predictive performance across episodes for the Lorenz 96 model. The prequential posterior (orange curve) improves with additional data, while the misspecified EnKF (blue curve) shows little change, as measured by calibration error, normalised RMSE, and coefficient of determination R^2 . The green dotted line represents the maximum achievable value for each metric. In the top panel, diagnostics are computed on the next episode (of length $\tau = 100$) of the same dataset, while the bottom panel uses a separate test dataset (of length 2000).

4.2 WeatherBench

The WeatherBench dataset (Rasp et al., 2020) is an open-source benchmark for data-driven weather forecasting. It provides hourly measurements of various atmospheric fields from 1979 to 2018 at multiple spatial resolutions. In this work, we select a resolution of 5.625° in both longitude and latitude, corresponding to a 32×64 grid, and focus on an 8×16 subset covering the European subregion. We use one observation per day (12:00 UTC) of the 500 hPa geopotential height (Z500) field. Our forecasting task is to predict one day ahead using the previous three daily observations. The period 1979 – 1998 is used for training, and calibration tests are conducted on the 1999 – 2002 data.

The deep generative forecasting model (DGFN) We adopt a U-Net architecture (Ronneberger et al., 2015) for the generative network, following the adaptation in Pacchiardi et al. (2024a). This encoder–decoder structure processes the input through successive encoder layers, each producing a downsampled latent representation. The final encoder output is passed to a bottleneck layer, which preserves the scale while transforming the features. The decoder then progressively upsamples this representation, with skip connections linking encoder and decoder layers at the same resolution. These connections ensure that both large-scale structures and fine-scale details contribute to the output. A random noise is drawn from standard Gaussian distribution and added to the bottleneck representation before decoding.

Empirical findings For the WeatherBench experiment, we again infer prequential posteriors after each observation episode and evaluate predictive skill on the test set using calibration error, NRMSE, and R^2 . As shown in Figure 3, assimilating additional episodes leads to a steady reduction in calibration error and normalized RMSE, while R^2 rises toward unity, demonstrating consistent improvements in forecast accuracy and calibration over the posterior updates. Although a more complex generative model could potentially achieve optimal performance. Our results show that the current model reaches its best predictive accuracy with sufficient training data. In Figure 4, we present sample predictions from the final posterior predictive distribution for a test-set observation. The simulated fields closely reproduce the underlying spatial structure.

5 Conclusion

In this work, we proposed a scalable and likelihood-free Bayesian framework for data assimilation in deep generative models, with a focus on improving probabilistic forecasting as new data becomes available. To address the challenge posed by intractable likelihoods, we adopted a generalized Bayesian approach based on the prequential loss, which allows for posterior updating without requiring explicit access to a likelihood function. This framework is particularly suitable for sequential learning and forecasting in temporally dependent settings. We also adopted an alternative notion of consistency, originally proposed by Dawid; which is appropriate under model misspecification. Rather than assuming the existence of a true parameter, we focus on identifying parameters that minimize predictive risk, thus aligning model training with the ultimate goal of forecasting accuracy. For posterior sampling, we implemented a waste-free sequential Monte Carlo (SMC) algorithm, augmented with a stochastic gradient MCMC (SGMCMC)–style forward kernel. To further enhance efficiency

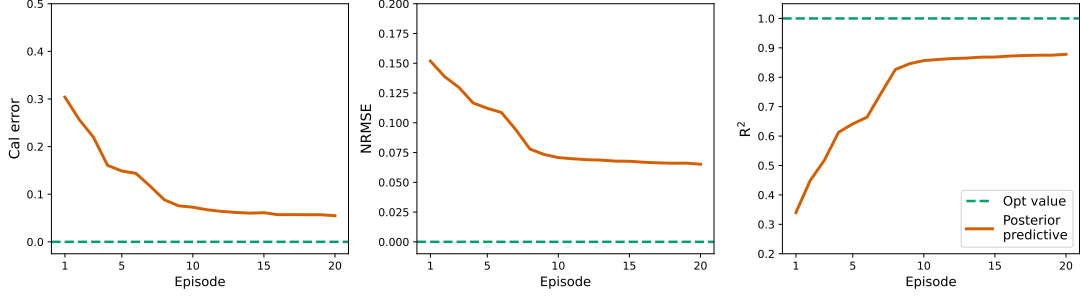


Figure 3: Data assimilation for DGFM on the European subset of the WeatherBench dataset. We infer the prequential posteriors after each episode (~ 1 year) and plot the diagnostics computed on a separate test data (~ 4 years). The orange curve shows the value of the the calibration metrics (calibration error, NRMSE, R^2) of the posterior predictives obtained after each assimilation episode and the predictive performance of the posteriors improve steadily over each training episode. The green dotted line represents the maximum achievable value for each metric. Steady decay of the calibration error and NRMSE curves, along with the upward trend of the R^2 curve indicates effective data assimilation via posterior parameter updates in DGFM.

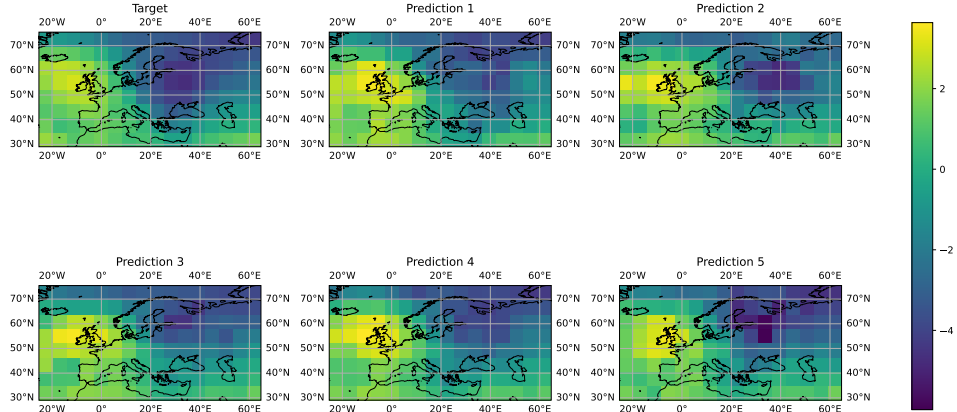


Figure 4: Comparison of target and simulations. The top left image shows an observation from the year 2000, while the remaining five images are simulated from the posterior predictive distributions generated from the final posterior predictive distribution. The simulations roughly capture the underlying spatial pattern.

in high-dimensional settings, we employed adaptive preconditioning inspired by optimization techniques such as RMSprop. The resulting approach is scalable, parallelizable, and well-suited for training complex models like neural networks.

We demonstrated the effectiveness of our approach on both a nonlinear time series model (Lorenz 96) and a meteorological image forecasting task (WeatherBench), highlighting its potential for real-world forecasting applications such as digital twin systems Sharma et al. (2022). For Lorenz 96, we compared our method against an ensemble Kalman filter with a commonly used misspecified state-space model for the system. We showed that our approach progressively learns an effective representation of the underlying dynamics, ultimately achieving superior predictive accuracy. This illustrates that when the true state-space model is unknown, the Kalman filter struggles, whereas our method can still perform considerably well. More broadly, in settings where an appropriate state-space model is unavailable or computationally prohibitive, our framework offers a practical model-updating mechanism. Its predictive strength follows from the universal approximation property of deep neural networks, which ensures that with sufficient data, the learned simulator can approximate the relevant physical relationships and deliver reliable forecasts.

Promising future directions include a more rigorous treatment of the approximation error introduced by the forward Markov kernel, as well as an analysis of the error bounds associated with the waste-free SMC procedure. Additionally, while we have used Gaussian and Student- t priors for the neural network parameters, exploring structured or shrinkage priors may further improve performance by introducing beneficial regularization in overparameterized settings.

References

Z. An, D. J. Nott, and C. Drovandi. Robust Bayesian synthetic likelihood via a semi-parametric approach. *Statistics and Computing*, 30(3):543–557, 2020.

E. Andersson, J. Pailleux, J.-N. Thépaut, J. Eyre, A. McNally, G. Kelly, and P. Courtier. Use of cloud-cleared radiances in three/four-dimensional variational data assimilation. *Quarterly Journal of the Royal Meteorological Society*, 120(517):627–653, 1994.

R. Arcucci, J. Zhu, S. Hu, and Y.-K. Guo. Deep data assimilation: integrating deep learning with data assimilation. *Applied Sciences*, 11(3):1114, 2021.

E. Bernton, P. E. Jacob, M. Gerber, and C. P. Robert. Approximate Bayesian computation with the Wasserstein distance. *Journal of the Royal Statistical Society Series B: Statistical Methodology*, 81(2):235–269, 2019.

K. Bi, L. Xie, H. Zhang, X. Chen, X. Gu, and Q. Tian. Pangu-Weather: A 3d high-resolution model for fast and accurate global weather forecast, 2022. URL <https://arxiv.org/abs/2211.02556>.

P. G. Bissiri, C. C. Holmes, and S. G. Walker. A general framework for updating belief distributions. *Journal of the Royal Statistical Society: Series B (Statistical Methodology)*, 78(5):1103–1130, 2016.

C. Chen, D. Carlson, Z. Gan, C. Li, and L. Carin. Bridging the gap between stochastic gradient MCMC and stochastic optimization. In *Artificial Intelligence and Statistics*, pages 1051–1060. PMLR, 2016.

T. Chen, E. Fox, and C. Guestrin. Stochastic gradient Hamiltonian Monte Carlo. In *International conference on machine learning*, pages 1683–1691. PMLR, 2014.

P. Courtier, E. Andersson, W. Heckley, D. Vasiljevic, M. Hamrud, A. Hollingsworth, F. Rabier, M. Fisher, and J. Pailleux. The ECMWF implementation of three-dimensional variational assimilation (3D-Var). i: Formulation. *Quarterly Journal of the Royal Meteorological Society*, 124(550):1783–1807, 1998.

H.-D. Dau and N. Chopin. Waste-free sequential Monte Carlo. *Journal of the Royal Statistical Society Series B: Statistical Methodology*, 84(1):114–148, 2022.

A. P. Dawid. Present position and potential developments: Some personal views statistical theory the prequential approach. *Journal of the Royal Statistical Society: Series A (General)*, 147(2):278–290, 1984.

A. P. Dawid. Fisherian inference in likelihood and prequential frames of reference. *Journal of the Royal Statistical Society: Series B (Methodological)*, 53(1):79–100, 1991.

A. P. Dawid. Prequential data analysis. *Lecture Notes-Monograph Series*, pages 113–126, 1992.

A. P. Dawid and A. Tewari. On learnability under general stochastic processes. *arXiv preprint arXiv:2005.07605*, 2020.

A. P. Dawid and V. G. Vovk. Prequential probability: principles and properties. *Bernoulli*, pages 125–162, 1999.

P. Del Moral, A. Doucet, and A. Jasra. Sequential Monte Carlo samplers. *Journal of the Royal Statistical Society Series B: Statistical Methodology*, 68(3):411–436, 2006.

N. Ding, Y. Fang, R. Babbush, C. Chen, R. D. Skeel, and H. Neven. Bayesian sampling using stochastic gradient thermostats. *Advances in neural information processing systems*, 27, 2014.

G. Duran-Martin, M. Altamirano, A. Y. Shestopaloff, L. Sánchez-Betancourt, J. Knoblauch, M. Jones, F.-X. Briol, and K. Murphy. Outlier-robust Kalman filtering through generalised Bayes. *arXiv preprint arXiv:2405.05646*, 2024.

R. Dutta, J. Corander, S. Kaski, and M. U. Gutmann. Likelihood-free inference by ratio estimation. *arXiv preprint arXiv:1611.10242*, 2016.

G. Evensen. The ensemble Kalman filter: Theoretical formulation and practical implementation. *Ocean dynamics*, 53(4):343–367, 2003.

M. Fisher, J. Nocedal, Y. Trémolet, and S. J. Wright. Data assimilation in weather forecasting: a case study in PDE-constrained optimization. *Optimization and Engineering*, 10(3):409–426, 2009.

A. R. Gallant and H. White. A unified theory of estimation and inference for nonlinear dynamic models. *(No Title)*, 1988.

M. Girolami and B. Calderhead. Riemann manifold Langevin and Hamiltonian Monte Carlo methods. *Journal of the Royal Statistical Society Series B: Statistical Methodology*, 73(2):123–214, 2011.

T. Gneiting and A. E. Raftery. Strictly proper scoring rules, prediction, and estimation. *Journal of the American statistical Association*, 102(477):359–378, 2007.

J. Jewson, J. Q. Smith, and C. Holmes. Principles of Bayesian inference using general divergence criteria. *Entropy*, 20(6):442, 2018.

A. Jones and B. Leimkuhler. Adaptive stochastic methods for sampling driven molecular systems. *The Journal of chemical physics*, 135(8), 2011.

J. Knoblauch, J. Jewson, and T. Damoulas. An optimization-centric view on bayes’ rule: Reviewing and generalizing variational inference. *Journal of Machine Learning Research*, 23(132):1–109, 2022.

R. Lam, A. Sanchez-Gonzalez, M. Willson, P. Wirnsberger, M. Fortunato, F. Alet, S. Ravuri, T. Ewalds, Z. Eaton-Rosen, W. Hu, A. Merose, S. Hoyer, G. Holland, O. Vinyals, J. Stott, A. Pritzel, S. Mohamed, and P. Battaglia. GraphCast: Learning skillful medium-range global weather forecasting, 2023. URL <https://arxiv.org/abs/2212.12794>.

S. Lang, M. Alexe, M. C. A. Clare, C. Roberts, R. Adewoyin, Z. B. Bouallègue, M. Chantry, J. Dramsch, P. D. Dueben, S. Hahner, P. Maciel, A. Prieto-Nemesio, C. O’Brien, F. Pinault, J. Polster, B. Raoult, S. Tietsche, and M. Leutbecher. AIFS-CRPS: Ensemble forecasting using a model trained with a loss function based on the continuous ranked probability score, 2024. URL <https://arxiv.org/abs/2412.15832>.

B. Leimkuhler and X. Shang. Adaptive thermostats for noisy gradient systems. *SIAM Journal on Scientific Computing*, 38(2):A712–A736, 2016.

J. Lintusaari, M. U. Gutmann, R. Dutta, S. Kaski, and J. Corander. Fundamentals and recent developments in approximate Bayesian computation. *Systematic Biology*, 66(1):e66–e82, 2017.

E. N. Lorenz. Predictability: A problem partly solved. In *Proc. Seminar on predictability*, volume 1, pages 1–18. Reading, 1996.

J. E. Matheson and R. L. Winkler. Scoring rules for continuous probability distributions. *Management science*, 22(10):1087–1096, 1976.

J. W. Miller. Asymptotic normality, concentration, and coverage of generalized posteriors. *Journal of Machine Learning Research*, 22(168):1–53, 2021.

A. H. Murphy and R. L. Winkler. Scoring rules in probability assessment and evaluation. *Acta psychologica*, 34:273–286, 1970.

T. Nguyen, J. Brandstetter, A. Kapoor, J. K. Gupta, and A. Grover. ClimaX: A foundation model for weather and climate. In A. Krause, E. Brunskill, K. Cho, B. Engelhardt, S. Sabato, and J. Scarlett, editors, *Proceedings of the 40th International Conference on Machine Learning*, volume 202 of *Proceedings of Machine Learning Research*, pages 25904–25938. PMLR, 23–29 Jul 2023. URL <https://proceedings.mlr.press/v202/nguyen23a.html>.

L. Pacchiardi, R. Adewoyin, P. Dueben, and R. Dutta. Probabilistic forecasting with generative networks via scoring rule minimization. *Journal of Machine Learning Research*, 25:1–64, 2024a.

L. Pacchiardi, S. Khoo, and R. Dutta. Generalized Bayesian likelihood-free inference. *Electronic Journal of Statistics*, 18(2):3628–3686, 2024b.

J. Pathak, S. Subramanian, P. Harrington, S. Raja, A. Chattopadhyay, M. Mardani, T. Kurth, D. Hall, Z. Li, K. Azizzadenesheli, P. Hassanzadeh, K. Kashinath, and A. Anandkumar. FourCastNet: A global data-driven high-resolution weather model using adaptive Fourier neural operators, 2022. URL <https://arxiv.org/abs/2202.11214>.

I. Price, A. Sanchez-Gonzalez, F. Alet, T. R. Andersson, A. El-Kadi, D. Masters, T. Ewalds, J. Stott, S. Mohamed, P. Battaglia, R. Lam, and M. Willson. GenCast: Diffusion-based ensemble forecasting for medium-range weather, 2024. URL <https://arxiv.org/abs/2312.15796>.

L. F. Price, C. C. Drovandi, A. Lee, and D. J. Nott. Bayesian synthetic likelihood. *Journal of Computational and Graphical Statistics*, 27(1):1–11, 2018.

Y. Qu, J. Nathaniel, S. Li, and P. Gentine. Deep generative data assimilation in multimodal setting. In *Proceedings of the IEEE/CVF Conference on Computer Vision and Pattern Recognition*, pages 449–459, 2024.

S. Rasp, P. D. Dueben, S. Scher, J. A. Weyn, S. Mouatadid, and N. Thuerey. Weather-Bench: a benchmark data set for data-driven weather forecasting. *Journal of Advances in Modeling Earth Systems*, 12(11):e2020MS002203, 2020.

M. I. Ribeiro. Kalman and extended Kalman filters: Concept, derivation and properties. *Institute for Systems and Robotics*, 43(46):3736–3741, 2004.

O. Ronneberger, P. Fischer, and T. Brox. U-net: Convolutional networks for biomedical image segmentation. In *International Conference on Medical image computing and computer-assisted intervention*, pages 234–241. Springer, 2015.

M. Roth, G. Hendeby, C. Fritzsche, and F. Gustafsson. The ensemble Kalman filter: a signal processing perspective. *EURASIP Journal on Advances in Signal Processing*, 2017(1), Aug. 2017. ISSN 1687-6180. doi: 10.1186/s13634-017-0492-x. URL <http://dx.doi.org/10.1186/s13634-017-0492-x>.

S. S. Roy, R. G. Everitt, C. P. Robert, and R. Dutta. Generalized Bayesian deep reinforcement learning. *arXiv preprint arXiv:2412.11743*, 2024.

L. J. Savage. Elicitation of personal probabilities and expectations. *Journal of the American Statistical Association*, 66(336):783–801, 1971.

A. Sharma, E. Kosasih, J. Zhang, A. Brintrup, and A. Calinescu. Digital twins: State of the art theory and practice, challenges, and open research questions. *Journal of Industrial Information Integration*, 30:100383, 2022.

K. Skouras. *On the optimal performance of forecasting systems: The prequential approach*. University of London, University College London (United Kingdom), 1998.

K. Skouras and A. P. Dawid. Consistency in misspecified models. *ReM search Report, Department of Statistical Science, University College London*, 2000.

G. J. Székely and M. L. Rizzo. A new test for multivariate normality. *Journal of Multivariate Analysis*, 93(1):58–80, 2005.

S. Vetra-Carvalho, P. J. Van Leeuwen, L. Nerger, A. Barth, M. U. Altaf, P. Brasseur, P. Kirchgessner, and J.-M. Beckers. State-of-the-art stochastic data assimilation methods for high-dimensional non-gaussian problems. *Tellus A: Dynamic Meteorology and Oceanography*, 70(1):1–43, 2018.

K. Waghmare and J. Ziegel. Proper scoring rules for estimation and forecast evaluation. *arXiv preprint arXiv:2504.01781*, 2025.

M. Welling and Y. W. Teh. Bayesian learning via stochastic gradient Langevin dynamics. In *Proceedings of the 28th international conference on machine learning (ICML-11)*, pages 681–688. Citeseer, 2011.

M. J. Werner, K. Ide, and D. Sornette. Earthquake forecasting based on data assimilation: sequential Monte Carlo methods for renewal point processes. *Nonlinear Processes in Geophysics*, 18(1):49–70, 2011.

H. White. *Estimation, inference and specification analysis*. Number 22. Cambridge university press, 1996.

R. L. Winkler. The quantification of judgment: Some methodological suggestions. *Journal of the American Statistical Association*, 62(320):1105–1120, 1967.

Y. Zhou, A. M. Johansen, and J. A. Aston. Toward automatic model comparison: an adaptive sequential Monte Carlo approach. *Journal of Computational and Graphical Statistics*, 25(3):701–726, 2016.

Appendix A.

A.1 Full statement of Lemma 3

[**Martingale uniform law of large numbers**] Let us consider the assumptions,

U1 The metric space (Θ, d) is compact.

U2 Suppose, $B(\theta, \rho)$ denotes a ball around θ of radius ρ and define

$$\underline{\ell}_t(\theta, \rho) = \inf_{s \in B(\theta, \rho)} \ell_t(s) \quad \text{and} \quad \bar{\ell}_t(\theta, \rho) = \sup_{s \in B(\theta, \rho)} \ell_t(s).$$

For any $\theta \in \Theta$ there is $\rho(\theta)$ such that for all $\rho < \rho(\theta)$ the sequence of random variables $(\bar{\ell}_t(\theta, \rho))$ and $(\underline{\ell}_t(\theta, \rho))$ satisfy pointwise strong martingale LLN's (with common denominator an increasing predictable sequence A_T).

U3 For all $\theta \in \Theta$, P -a.s.,

$$\lim_{\rho \rightarrow 0} \limsup_{T \geq 1} \frac{1}{A_T} \sum_{t=1}^T E_{t-1} \{ \bar{\ell}_t(\theta, \rho) - \underline{\ell}_t(\theta, \rho) \} = 0.$$

Lemma Suppose the assumptions **U1-U3** holds, then P -a.s.,

$$\sup_{\theta \in \Theta} \left| \frac{1}{A_T} \sum_{t=1}^T [l_t(\theta) - E_{t-1} l_t(\theta)] \right| \rightarrow 0.$$

Often, the assumptions **U2**, **U3** are difficult to verify. However, assumption **A2** implies **U2** and assumption **A3** implies **U3**, which are relatively easier to check.

A.2 Proof of Corollary 4

Corollary Under the assumptions **A1-A4**, it follows from Lemma 3 that,

$$\sup_{\theta \in \Theta} |\bar{L}_T(\theta) - \bar{L}^*(\theta)| \rightarrow 0 \text{ as } T \rightarrow \infty,$$

with probability one under P .

Proof Under assumption **A4**, for a fixed $\epsilon > 0$ there exists a $T_1(\epsilon)$ such that for all $T > T_1(\epsilon)$ with probability 1 under P ,

$$\begin{aligned} |\bar{L}_T^*(\theta) - \bar{L}^*(\theta)| &< \epsilon/2, \text{ for all } \theta \in \Theta \\ \implies \sup_{\theta \in \Theta} |\bar{L}_T^*(\theta) - \bar{L}^*(\theta)| &< \epsilon/2. \end{aligned} \tag{12}$$

Similarly, under assumptions **A1-A3**, Lemma 3 implies that for the fixed $\epsilon > 0$ there exists a $T_2(\epsilon)$ such that for all $T > T_2(\epsilon)$ with probability 1 under P ,

$$\sup_{\theta \in \Theta} |\bar{L}_T(\theta) - \bar{L}_T^*(\theta)| < \epsilon/2. \tag{13}$$

On combining equations 12 and 13, for any $T > \max\{T_1(\epsilon), T_2(\epsilon)\}$

$$\begin{aligned} \sup_{\theta \in \Theta} |\bar{L}_T(\theta) - \bar{L}^*(\theta)| &\leq \sup_{\theta \in \Theta} \{ |\bar{L}_T(\theta) - \bar{L}_T^*(\theta)| + |\bar{L}_T^*(\theta) - \bar{L}^*(\theta)| \} \\ &< \epsilon/2 + \epsilon/2 = \epsilon, \end{aligned} \tag{14}$$

with probability 1 under P . Since equation 14 holds for an arbitrary $\epsilon > 0$, it follows that, with probability 1 under P ,

$$\sup_{\theta \in \Theta} |\bar{L}_T(\theta) - \bar{L}^*(\theta)| \rightarrow 0 \text{ as } T \rightarrow \infty.$$

■

A.3 Lemma on the existence of an extremum estimator

Lemma *Let (Ω, \mathcal{F}) be a measurable space, and let (Θ, d) be a compact, separable space. Let $Q : \Omega \times \Theta \rightarrow \mathbb{R} \cup \{-\infty, \infty\}$ be such that $Q(\cdot, \theta)$ is \mathcal{F} -measurable for each θ in Θ , and $Q(\omega, \cdot)$ is continuous for all ω in an event $F \in \mathcal{F}$. Then, there exists a function $\hat{\theta} : \Omega \rightarrow \Theta$ such that $\hat{\theta}$ is \mathcal{F} -measurable and for all ω in F*

$$Q(\omega, \hat{\theta}(\omega)) = \inf_{\theta \in \Theta} Q(\omega, \theta).$$

A.4 Proof of Lemma 6

Lemma *(Asymptotic consistency) Under assumptions **A1-A7**, as $T \rightarrow \infty$, we have with probability 1 under P ,*

$$d(\hat{\theta}_T, \theta^*) \rightarrow 0.$$

We present here a proof of the lemma based on Theorem 5.1 in Skouras (1998) as adapted by Pacchiardi et al. (2024a).

Proof From assumption **A7**, for a fixed $\epsilon > 0$ it is possible to find a $\delta(\epsilon) > 0$ such that,

$$\min_{\theta: d(\theta, \theta^*) \geq \epsilon} \bar{L}^*(\theta) - \bar{L}^*(\theta^*) = \delta(\epsilon), \quad (15)$$

with probability 1 under P .

Due to Corollary 4, with probability 1 under P , there exists a $T_1(\delta(\epsilon))$ such that for all $T > T_1(\delta(\epsilon))$

$$|\bar{L}_T(\theta^*) - \bar{L}^*(\theta^*)| < \delta(\epsilon)/2,$$

which implies

$$\begin{aligned} \bar{L}^*(\theta^*) &> \bar{L}_T(\theta^*) - \delta(\epsilon)/2 \\ &\geq \bar{L}_T(\hat{\theta}_T) - \delta(\epsilon)/2, \end{aligned} \quad (16)$$

where the second inequality is from the definition of $\hat{\theta}_T$.

On exploiting Corollary 4 once again, we can define a $T_2(\delta(\epsilon))$ such that for all $T > T_2(\delta(\epsilon))$

$$|\bar{L}_T(\hat{\theta}_T) - \bar{L}^*(\hat{\theta}_T)| < \delta(\epsilon)/2, \quad (17)$$

with probability 1 under P .

Then, with probability 1 under P , for all $T > \max\{T_1(\delta(\epsilon)), T_2(\delta(\epsilon))\}$

$$\begin{aligned}\bar{L}^*(\hat{\theta}_T) - \bar{L}^*(\theta^*) &= \bar{L}^*(\hat{\theta}_T) - \bar{L}_T(\hat{\theta}_T) + \bar{L}_T(\hat{\theta}_T) - \bar{L}^*(\theta^*) \\ &< \delta(\epsilon)/2 + \delta(\epsilon)/2 = \delta(\epsilon)\end{aligned}\tag{18}$$

from equation 16 and equation 17.

Note that equation 18 ensures that the difference considered in equation 15 is smaller than $\delta(\epsilon)$ when $\theta = \hat{\theta}_T$. However, by equation 15, the same difference is at least $\delta(\epsilon)$ for all θ that are outside the ϵ -radius ball around θ^* . This implies that, $\hat{\theta}_T$ must lie inside the ϵ -radius ball, meaning that $d(\hat{\theta}_T, \theta^*) < \epsilon$ with probability 1 under P . Since this is true for any $\epsilon > 0$, it follows that, with probability 1 under P

$$d(\hat{\theta}_T, \theta^*) \rightarrow 0 \text{ as } T \rightarrow \infty.$$

■

A.5 Sketch proof of Theorem 8

Proof From Lemma 6, we have, with probability one under P , as $T \rightarrow \infty$,

$$d(\hat{\theta}_T, \theta^*) \rightarrow 0.$$

which proves the existence of a sequence of estimators $\{\hat{\theta}_T\}_{T=1}^{\infty}$ such that as $T \rightarrow \infty$, with probability one under P , $d(\hat{\theta}_T, \theta^*) \rightarrow 0$ under the assumptions **A1-A7**.

By Theorem 6 from Miller (2021), using the above sequence of estimators $\{\hat{\theta}_T\}_{T=1}^{\infty}$ along with the assumptions **A9-A11**, $L_T(\theta)$ can be represented as,

$$\bar{L}_T(\theta) = \bar{L}_T(\hat{\theta}_T) + \frac{1}{2}(\theta - \hat{\theta}_T)'H_T(\theta - \hat{\theta}_T) + r_T(\theta - \hat{\theta}_T)\tag{19}$$

where $H_T = \bar{L}_T''(\hat{\theta}_T) \in \mathbb{R}^{p \times p}$ is symmetric and $H_T \rightarrow H^*$. There exists $\epsilon_0, c_0 > 0$ such that, for all T sufficiently large, for all $\theta \in B_{\epsilon_0}(\mathbf{0})$, we have $|r_T(\theta)| \leq c_0|\theta|^3$.

Finally, on using the Taylor series expansion of the function $\bar{L}_T(\theta)$ in equation 19, together with the assumptions **A8** and **A12**, the Theorem 8 holds (by Theorem 4 from Miller (2021)).

For completeness, Theorems 4 and 6 from Miller (2021) are restated below as Theorems 9 and 10, respectively.

■

Theorem 9 [Adapted from Theorem 4 from Miller (2021)] Fix $\theta^* \in \mathbb{R}^p$ and let $\pi : \mathbb{R}^p \rightarrow \mathbb{R}$ be a probability density with respect to Lebesgue measure such that π is continuous at θ^* and $\pi(\theta^*) > 0$. Let $\bar{L}_T : \mathbb{R}^p \rightarrow \mathbb{R}$ for $T \in \mathbb{N}$ and assume:

M1 \bar{L}_T can be represented as

$$\bar{L}_T(\theta) = \bar{L}_T(\hat{\theta}_T) + \frac{1}{2}(\theta - \hat{\theta}_T)'H_T(\theta - \hat{\theta}_T) + r_T(\theta - \hat{\theta}_T)$$

where $\hat{\theta}_T \in \mathbb{R}^p$ such that $\hat{\theta}_T \rightarrow \theta^*$, $H_T \in \mathbb{R}^{p \times p}$ symmetric such that $H_T \rightarrow H^*$ for some positive definite H^* , and $r_T : \mathbb{R}^p \rightarrow \mathbb{R}$ has the following property: there exist $\varepsilon_0, c_0 > 0$ such that for all T sufficiently large, for all $\theta \in B_{\varepsilon_0}(\mathbf{0})$, we have $|r_T(\theta)| \leq c_0|\theta|^3$;

M2 For any $\varepsilon > 0$, $\liminf_T \inf_{\theta \in B_\varepsilon(\hat{\theta}_T)^c} (\bar{L}_T(\theta) - \bar{L}_T(\hat{\theta}_T)) > 0$,

then defining $z_T = \int_{\Theta} \exp(-L_T(\theta)) \pi(\theta) d\theta$ and $\pi_P(\theta|y^T) = \pi(\theta) \exp(-L_T(\theta))/z_T$ we have,

$$\int_{B_\epsilon(\theta^*)} \pi_P(\theta|y^T) d\theta \xrightarrow{T \rightarrow \infty} 1 \quad \text{for all } \epsilon > 0,$$

which means, $\pi_P(\theta|y^T)$ concentrates at θ^* ;

$$z_T \approx \frac{\exp(-L_T(\hat{\theta}_T)) \pi(\theta^*)}{|\det H^*|^{1/2}} \left(\frac{2\pi}{A_T} \right)^{p/2}$$

as $T \rightarrow \infty$ (Laplace approximation), and letting q_T be the density of $\sqrt{A_T}(\theta - \hat{\theta}_T)$ when $\theta \sim \pi_{GP}(\theta|y^T)$,

$$\int_{\Theta} |q_T(\theta) - \mathcal{N}(\theta | \mathbf{0}, H^{*-1})| d\theta \xrightarrow{T \rightarrow \infty} 0,$$

which implies, q_T converges to $\mathcal{N}(\mathbf{0}, H^{*-1})$ in total variation.

Note that, we use A_T instead of T as in Theorem 4 from Miller (2021). Since any A_T satisfying Assumption **A2** is an increasing function of T , Theorem 9 continues to hold for such choices of A_T . This connection is crucial for extending the Bernstein-von Mises result in our setting, and we therefore apply Theorem 9 to ultimately derive Theorem 8.

Theorem 10 [Adapted from Theorem 6 from Miller (2021)] Let $E \subseteq \mathbb{R}^p$ be open and convex, and let $\theta^* \in E$. Let $\bar{L}_T : E \rightarrow \mathbb{R}$ have continuous third derivatives, and assume:

M3 there exist $\hat{\theta}_T \in E$ such that $\hat{\theta}_T \rightarrow \theta^*$ and $\bar{L}'_T(\hat{\theta}_T) = 0$ for all T sufficiently large,

M4 $\bar{L}''_T(\theta^*) \rightarrow H^*$ as $T \rightarrow \infty$ for some positive definite H^* , and

M5 \bar{L}'''_T is uniformly bounded;

Then, letting $H_T = \bar{L}''_T(\hat{\theta}_T)$, condition **M1** of Theorem 9 is satisfied for all T sufficiently large.

Appendix B.

B.1 Choice of prior distribution for SMC

For both the Lorenz 96 and WeatherBench experiments, we set the initial proposal distribution equal to the prior distribution in the SMC procedure. We investigated the effect of different priors; specifically, a standard Gaussian and Student's t distributions with 3 and 5 degrees of freedom, on our inference results. Since the t_1 and t_2 distributions do not have a well-defined variance, we did not consider them. Figures 5 and 6 show that, although all priors exhibit similar trends in predictive accuracy across calibration error, NRMSE, and R^2 , the Gaussian prior converges faster. Therefore, we report the Gaussian prior results in the main text.

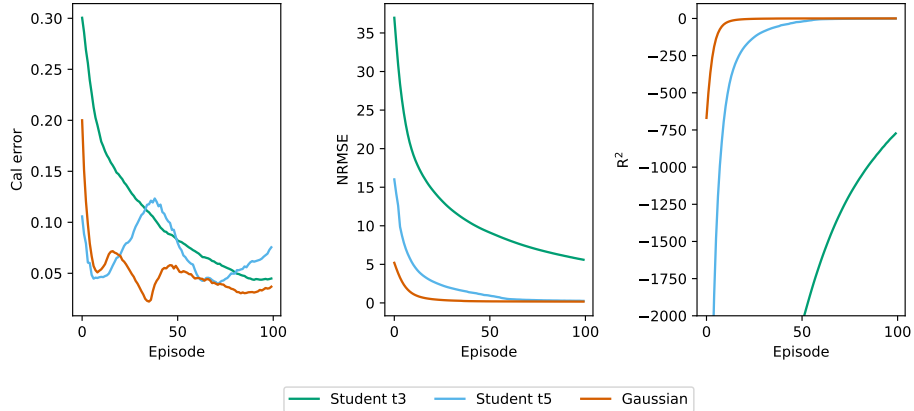


Figure 5: Predictive performance of the posterior predictives for the Lorenz 96 model under different SMC prior distributions. Calibration error, NRMSE, and R^2 are shown for three priors: a standard Gaussian (orange curve), a Student's t distribution with 3 degrees of freedom (green curve), and a Student's t distribution with 5 degrees of freedom (blue curve). All priors exhibit similar overall trends, but the Gaussian prior converges noticeably faster.

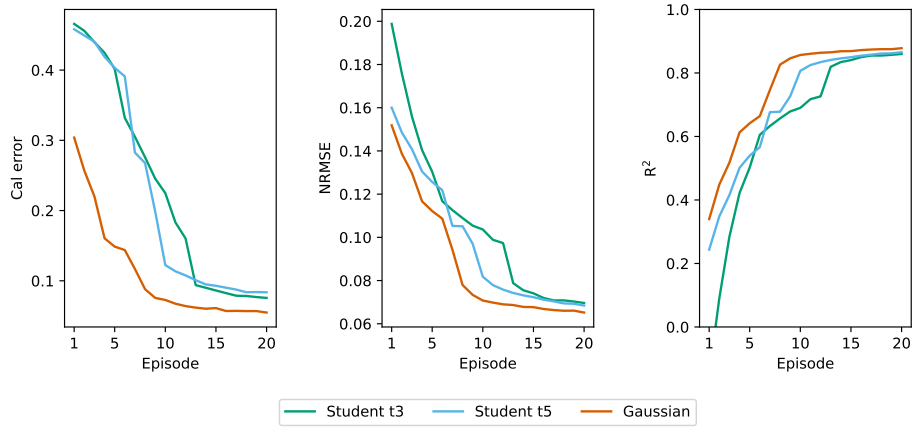


Figure 6: Predictive performance of the posterior predictives for the WeatherBench example under different SMC prior distributions. Calibration error, NRMSE, and R^2 are shown for three priors: a standard Gaussian (orange curve), a Student's t distribution with 3 degrees of freedom (green curve), and a Student's t distribution with 5 degrees of freedom (blue curve). All priors show similar overall trends, but the Gaussian prior converges slightly faster.

B.2 Details of the sampling scheme

Here we provide the values of hyperparameters used for sampling in Table 1.

Hyperparameter	Value
Learning rate, η	10^{-6}
Kernel parameter, σ	0.99
Kernel parameter, λ	10^{-8}
Initial momentum, α_0	$10^{-2} \cdot 1$
CESS threshold	$0.5 \cdot N = 75$

Table 1: Table containing hyperparameter values

B.3 Performance measures for probabilistic forecast

B.3.1 CALIBRATION ERROR

Here we consider a measure of calibration of a probabilistic forecast; this measure considers the univariate marginals of the probabilistic forecast distribution $Q^\theta(\cdot | \mathbf{y}_{t-k:t-1})$; for component i , let us denote that by $Q^{\theta,i}(\cdot | \mathbf{y}_{t-k:t-1})$.

The calibration error quantifies how well the credible intervals of the probabilistic forecast $Q^{\theta,i}(\cdot | \mathbf{y}_{t-k:t-1})$ match the distribution of the verification $Y_{t,i}$. Specifically, let $\alpha^*(i)$ be the proportion of times the verification $y_{t,i}$ falls into an α -credible interval of $Q^{\theta,i}(\cdot | \mathbf{y}_{t-k:t-1})$, computed over all values of t . If the marginal forecast distribution is perfectly calibrated for component i , $\alpha^*(i) = \alpha$ for all values of $\alpha \in (0, 1)$.

We define therefore the calibration error as the median of $|\alpha^*(i) - \alpha|$ over 100 equally spaced values of $\alpha \in (0, 1)$. Therefore, the calibration error is a value between 0 and 1, where 0 denotes perfect calibration.

B.3.2 NORMALIZED RMSE

We first introduce the Root Mean-Square Error (RMSE) as

$$\text{RMSE} = \sqrt{\frac{1}{T-k} \sum_{t=k+1}^T (\hat{y}_t - y_t)^2}$$

where we consider here for simplicity $t = k+1, \dots, T$. From the above, we obtain the Normalized RMSE (NRMSE) as

$$\text{NRMSE} = \frac{\text{RMSE}}{\max_t \{y_t\} - \min_t \{y_t\}}$$

NRMSE = 0 means that $\hat{y}_t = y_t$ for all t 's and means a perfect fit to the observed data.

B.3.3 COEFFICIENT OF DETERMINATION

The coefficient of determination R^2 measures how much of the variance in $\{y_t\}_{t=k+1}^T$ is explained by $\{\hat{y}_t\}_{t=k+1}^T$. Specifically, it is given by

$$R^2 = 1 - \frac{\sum_{t=k+1}^T (y_t - \hat{y}_t)^2}{\sum_{t=k+1}^N (y_t - \bar{y})^2},$$

where $\bar{y} = \frac{1}{T-k} \sum_{t=k+1}^T y_t$. $R^2 \leq 1$ and, when $R^2 = 1$, $\hat{y}_t = y_t$ for all t 's. Notice how R^2 is unbounded from below, and can thus be negative.